

Low Density *LH* Transition Triggered by Counter-NBI in the TUMAN-3M Tokamak

S.V. Lebedev¹, L.G. Askinazil, F.V. Chernyshev¹, V.E. Golant¹, M.A. Irzak¹,
V.A. Kornev¹, S.V. Krikunov¹, A.D. Melnik¹, D.V. Razumenko¹, V.V. Rozhdestvensky¹,
A.A. Rushkevich², A.I. Smirnov¹, A.S. Tukachinsky¹, M.I. Vild'junas¹, N.A. Zhubr¹
1 Ioffe Physico-Technical Institute, RAS, 194021, St Petersburg, RUSSIA
2 SPb State Polytechnical University, St Petersburg, RUSSIA

Threshold power needed to attain *H*-mode in a tokamak is a critical parameter for designing of future devices and in particular fusion reactor ITER [1]. According to commonly accepted scaling [2] the threshold power P_{thr} increases with average density \bar{n}_e when the density exceeds some $\bar{n}_{e,min}$ at which P_{thr} is minimal. The increase in P_{thr} with density imposes restrictions on *H*-mode accessibility in ITER at high density with planned auxiliary power, thus pushing forward concept of *H*-mode transition at lower density. On the other hand an increase in the P_{thr} towards low density, which is observed in many experiments [3,4,5,6], prevents the transition at lower \bar{n}_e as well. Physics of the threshold power increase at low \bar{n}_e is not well understood. Since the radial electric field E_r and $E_r \times B$ sheared flow play important roles in the *LH* transition one could expect these quantities effect the low \bar{n}_e transitions. Toroidal rotation and radial electric field generation during counter-NBI have been studied in [7] and recently reconsidered theoretically in [8]. Thus, motivation for the presented study is to analyze effect of counter-NBI on the *LH* transition at low density.

H-mode operational domain in the TUMAN-3M

In the TUMAN-3M ($R_0=0.53$ m, $a_l=0.22$ m, $B_T < 0.9$ T) the *H*-mode operational domain has a low density boundary of $(1.2 \div 1.4) \cdot 10^{19} \text{ m}^{-3}$, as indicated by vertical solid line in

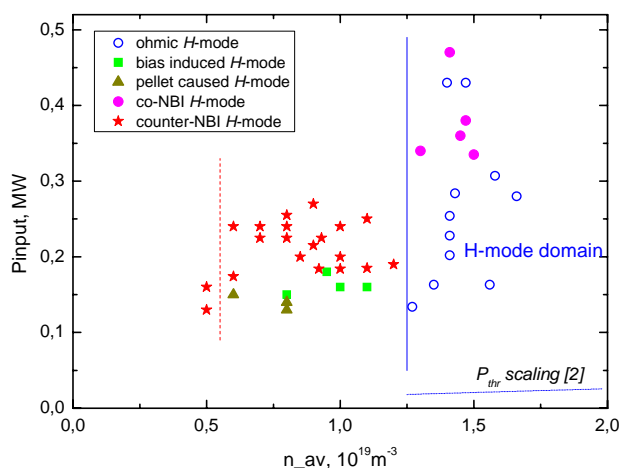


Fig.1. No transitions have been observed at densities below the boundary in ohmic and co-NBI heating schemes [9,10]. Relatively high input power should be noticed: P_{input} is

Fig.1. Input power as a function of average density at the *LH* transition time in various operational modes in TUMAN-3M. Vertical lines indicate density boundary for *LH* transitions: solid line – ohmic and co-NBI, dotted line – counter-NBI heated plasmas.

by a factor of 6-20 higher than the threshold estimations from scaling [2]. In the H -modes produced with assistance of electrode bias or shallow pellet evaporation (squares and triangles on Fig.1), the transition have been observed at \bar{n}_e down to $(0.6\div 1.0)\cdot 10^{19} \text{ m}^{-3}$ [11]. According to [11] in these cases an artificial E_r could help transition at lower density.

In the recent experiments on NB injection in the counter-current direction ($B_T=0.68 \text{ T}$, $I_p=140 \text{ kA}$, $E_0=20 \text{ keV}$) the H -mode transition at target density as low as $0.5\cdot 10^{19} \text{ m}^{-3}$ has been found (stars in Fig.1). Typical example of the discharge with the transition is presented in Fig.2. The transition occurred shortly after counter-NBI switch-on and is definitively linked to NBI application. Density and D_α traces in Fig.2 indicate substantial increase in the particle confinement time. Two-fold increase in the energy confinement time was deduced from diamagnetic measurements. It is unlikely that the increase in the absorbed power ΔP_{abs} causes the transition, since: (1) according to ASTRA transport simulations in the counter-NBI scenario $\Delta P_{\text{abs}}(\text{NBI})$ is small ($< 20 \text{ kW} \approx 10\% P_{\text{OHM}}$), (2) co-NBI does not trigger the transition at low \bar{n}_e even with $\Delta P_{\text{abs}}(\text{NBI}) = 200 \text{ kW} \approx P_{\text{OHM}}$. Thus, other reason allows the density boundary to move towards lower \bar{n}_e . The effect of NBI direction on the LH threshold power has been reported recently [12].

Measurements of plasma potential and toroidal rotation

In order to get an idea on radial electric field evolution in the above scenario the Heavy Ion Beam Probe diagnostic was employed. HIBP setup was chosen to follow central plasma potential $\Delta\Phi(0)$. The potential drop of up to 400 V was found in the counter-NBI heating scheme, see Fig.3. The measurement allows estimating $E_r \approx \Delta\Phi/(a_i/2) \approx 4\cdot 10^3 \text{ V/m}$. The estimation gives lower value for E_r , based on assumption of uniform E_r distribution within outer half of minor radius. It should be mentioned that H -mode transition itself (without influence of counter-NB injection) results in some drop in the potential. Example of the potential behavior during the ohmic H -mode transition is given in Fig.4. Here, the

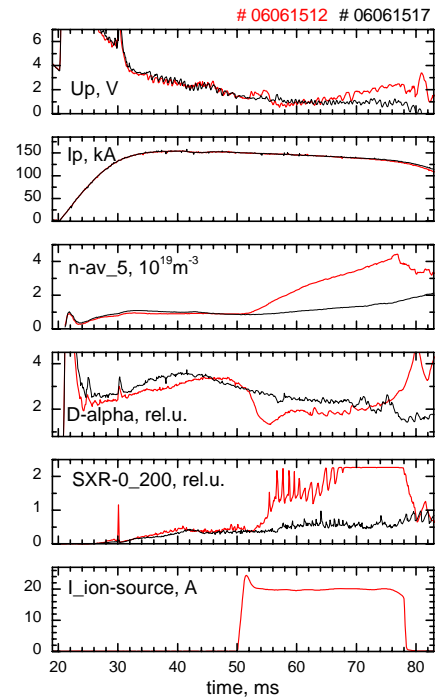


Fig.2. Example of the H -mode transition (shot #06061512) triggered by counter-NBI at density $0.8\cdot 10^{19} \text{ m}^{-3}$. Shot #06061517 – w/o NBI. Top to bottom: loop voltage, plasma current, density, D_α emission, soft X-ray radiation and ion source current (indicative of NBI duration).

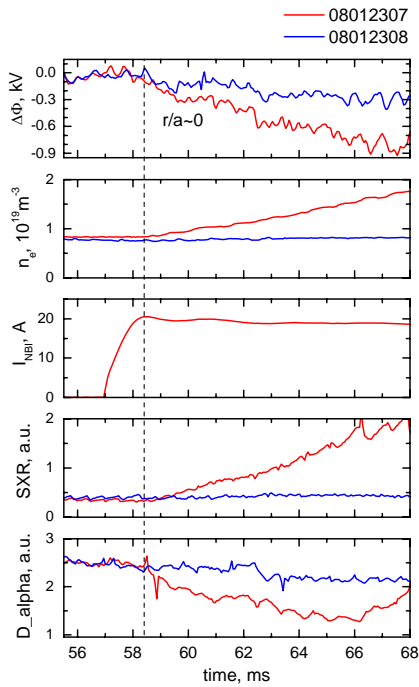


Fig.3. Evolution of plasma potential measured in the shots with low density LH transition in the presence of counter NBI (# 08012307) and w/o transition (# 08012308). Top to bottom: core potential, average density, ion source current, soft X-Ray radiation, D_α emission.

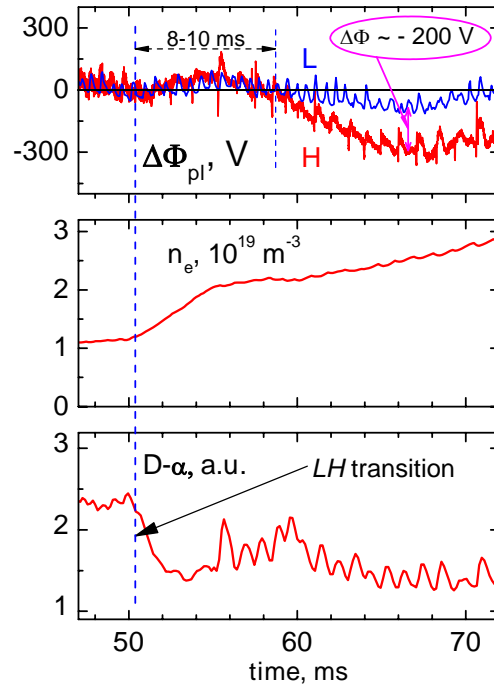
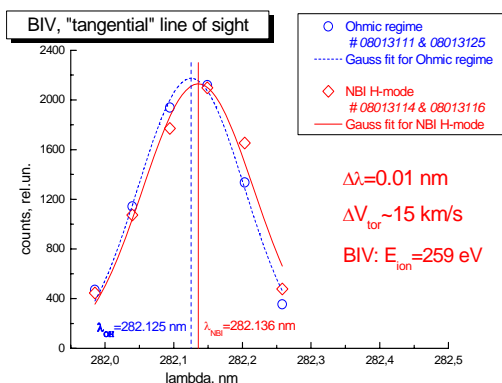


Fig.4. Evolution of plasma potential measured in the ohmic H-mode (red curve) and in the ohmic L-mode (blue curve). Top to bottom: core potential, average density, D_α emission. Notice, the drop in the potential is lower than in counter NBI scenario, shown on Fig3.

potential drop is substantially lower: 200 V and, contrary to NBI case, appears with noticeable delay of approximately 8-10 ms. Difference in the $\Delta\Phi(0)$ evolution in two scenarios suggest the direct effect of counter-NBI on the core plasma potential and possibly on the radial electric field.

Doppler spectroscopy was used for measurement of toroidal velocity V_ϕ of Boron and Carbon impurity ions (BIV line: $\lambda=282,2$ nm and CIII line: $\lambda=464,7$ nm). According to our estimations maximum brightness of BIV is located at $r = 0.6a$ and maximum brightness of CIII is nearby $0.9a$. Thus, the measured shifts provide data on V_ϕ in corresponding locations. Performed measurement has shown 15 km/s increase in the BIV torodal velocity in the counter-current direction following NBI application, see Fig.5, and negligible effect on CIII



toroidal velocity. The data might be considered as indication of bell-shaped radial distribution of toroidal velocity. If that's the case the central velocity of up to 30 km/s might be expected.

Fig.5. Measurement of toroidal velocity using Doppler spectroscopy of BIV line ($\lambda=282,2$ nm). Increase in the toroidal velocity of 15 km/s have been detected.

Discussion and summary

Observations of plasma potential and toroidal rotation presented in the preceding section could be understood in the framework of the following model. Under the conditions of counter-NBI a large amount of fast ions is captured on unconfined orbits. Fast losses of the ions produce radial current, which in our case is ~ 10 A. Quasineutrality condition requires return current I_{ret} flowing in the opposite direction through the plasma. Ampere force $I_{ret} \times B_\theta$ results in torque generation in the counter-current direction. Arising toroidal rotation can be estimated using the following expression: $[I_{ret} \times B_\theta] \cdot \delta r = (m_i \cdot n \cdot V_{pl} \cdot V_\phi) / \tau_\phi$, where $\delta r = a - r_{FI}$, r_{FI} – average radius of capture points on unconfined orbits, V_{pl} – plasma volume, τ_ϕ – toroidal momentum confinement time. Assuming $\tau_\phi = \tau_E$ the estimation $V_\phi \approx 30$ km/s could be obtained, which is in reasonable agreement with the Doppler spectroscopy data. Presuming Lorentz force $V_\phi \times B_\theta$ is balanced by the radial electric field the estimation of $E_r = -5 \cdot 10^3$ V/m is obtained. This quantity agrees well with E_r obtained by HIBP measurement ($4 \cdot 10^3$ V/m).

Thus, the presented observations of the *LH* transitions at very low density (down to $0.5 \cdot 10^{19}$ m⁻³) in the counter-NBI experiment on TUMAN-3M agree with the suggested model of rotation and radial electric field generation in the presence of large ion orbit losses. Emerging radial electric field and possibly sheared rotation help *LH* transition at low density.

Acknowledgements

The work was supported by Federal Agency for Science and Innovations MES RF: State Contract # 02.518.11.7023 and Grant “Leading Scientific School” # 5149.2006.2 and by Russian Foundation for Basic Research: Grants # 07-02-01311 & 07-02-00276.

References

- [1] E.J.Doyle, et al, in “Progress in ITER Physics Basis”, NF, 47(2007), S18
- [2] ITER Physics Expert Groups, in “ITER Physics Basis, Chapter 2”, NF, 39(1999), 2175
- [3] F. Wagner, et al, PRL, 49(1982), 1408
- [4] K. Burrell, et al, PRL, 59(1987), 1432
- [5] F. Ryter, et al, PPCF, 36(1994), A99
- [6] S. Fielding, et al, IAEA, Seville, 1994, v.II, 29
- [7] J. Kim, et al, PPCF, 38(1996), 1479
- [8] A. Thyagaraja, et al, PoP, 14(2007), 112504
- [9] S.V. Lebedev, et al, PPCF, 38(1996), 1103
- [10] S.V. Lebedev, et al, FEC2006, Chengdu, EX/P3-15
- [11] L.G. Askinazi, et al, Phys.Fluids B, v.5 (1993), 2420
- [12] T.C. Luce, et al, FEC2006, Chengdu, PD-3